Zaib, A., *et al.*: Boundary-Layer Flow of a Cu-Water Nanofluid over a ...
THERMAL SCIENCE: Year 2019, Vol. 23, No. 1, pp. 295-306

295

BOUNDARY-LAYER FLOW OF A Cu-WATER NANOFLUID OVER A PERMEABLE SHRINKING CYLINDER WITH HOMOGENOUS-HETROGENOUS REACTIONS: Dual Solutions

by

Aurang ZAIB[a], Masood KHAN[b], and Sharidan SHAFIE[c]*

[a] Department of Mathematical Sciences,
Federal Urdu University of Arts, Science and Technology, Karachi, Pakistan
[b] Department of Mathematics, Quaid-i-Azam University, Islamabad, Pakistan
[c] Department of Mathematical Sciences, Faculty of Science, University of Technology Malaysia,
Skudai, Johor, Malaysia

This research addresses the axi-symmetric flow of a Cu-water nanofluid past a porous shrinking cylinder in the presence of homogeneous-heterogeneous reactions. Using a similarity transformation, the basic PDE's are converted into ODE's. The transformed equations are solved using bvp4c numerically from MATLAB for several values of the physical parameters. The physical impact of governing parameters on the velocity profile, temperature profile, concentration profile as well as the skin friction coefficient, $f''(0)$, and the heat transfer rate, $-\theta'(0)$, are discussed carefully. The results indicate that the multiple solutions only exist when a certain value of suction is implemented through the permeable cylinder. Further, the curvature parameter, γ, accelerates the boundary-layer separation.

Key words: *dual solutions, nanofluid, homogenous-hetrogenous reactions*

Introduction

In recent times, the rapid growth of the human society significantly depends on the resources of energy. Thus several scientists and researchers are attempting to develop the new resources of energy in order to make use of solar energy which is suitable and easily available for various heating processes in industries. Choi [1] was first to use the nanoparticle to increase the thermal conductivity of fluids and storage of energy. Nanofluid is a fluid that containing the suspension of a nanometer sized particles of oxides, metals, nitrides, carbides, or nanotubes in regular base fluid such as engine oil, ethylene glycol, water, *etc.* Nanofluids have higher thermal conductivity than the base fluids. Makinde and Aziz [2] investigated the viscous flow and heat transfer filled with nanofluid over a heated stretching surface. Mustafa *et al.* [3] investigate the stagnation-point flow with heat transfer of a nanofluid over a stretching surface. Hady *et al.* [4] studied the effect of thermal radiation on the flow with heat transfer past a non-linear stretching sheet of a nanofluid with wall temperature. Hamad and Ferdows [5] obtained the similarity solutions of the flow with heat transfer past a non-linear stretching sheet filled with nanofluid. The mix convection flow of a nanofluid near a stagnation-point towards a shrinking surface was studied by Das [6]. Ibrahim *et al.* [7] analyzed the MHD flow near a stagnation-point of a nanofluid over a stretch-

---

296

Zaib, A., *et al.*: Boundary-Layer Flow of a Cu-Water Nanofluid over a ...
THERMAL SCIENCE: Year 2019, Vol. 23, No. 1, pp. 295-306

ing surface. The MHD viscous flow near a stagnation-point of a nanofluid towards a stretching/shrinking sheet was examined by Mansur *et al.* [8]. Hayat *et al.* [9] studied the stagnation point flow of carbon nanotubes over a stretching cylinder in the presence of slip effects. Recently, Dhanai *et al.* [10] obtained the dual solutions of the MHD viscous flow with heat transfer of a nanofluid towards a non-linear permeable stretching/shrinking surface with viscous dissipation. Very recently, Faiza [11] investigated the boundary-layer flow of a Cu-water based nanofluid and heat transfer over a moving wedge with radiation effect and obtained the dual solutions.

Nowadays, the study of viscous flow with heat and mass transfer past a stretching/shrinking cylinder has been given a lot of attention by researchers because of its vast applications in various industrial and engineering processes. Such as rubber sheets, annealing, glass fiber production, paper production and many more. Wang [12] investigated the steady viscous flow outer side of a stretching hollow cylinder at rest immersed in an ambient fluid. Ishak *et al.* [13] analyzed the viscous flow with heat transfer past a stretching cylinder with suction/blowing. Mukhopadhyay [14] examined the effect of slip on the flow past a stretching cylinder with chemically reactive solute. In other paper, Mukhopadhyay [15] investigated the MHD boundary-layer flow and heat transfer over a stretching cylinder with partial slip effect. The effect of mass suction on the flow and heat transfer towards a shrinking cylinder was studied by Bhattacharyya [16]. Najib *et al.* [17] investigated the effect of chemical reaction on the flow with mass transfer near a stagnation point over a stretching/shrinking cylinder with chemical reaction. Hayat *et al.* [18] analyzed the effect of viscous dissipation on the flow of a Casson fluid past an inclined stretching cylinder with thermal radiation. Recently, Omar *et al.* [19] obtained the similarity solution of viscous flow near a stagnation point of a nanofluid towards a shrinking cylinder.

Homogeneous-heterogeneous reactions involve in various chemical reactive system such as biochemical, catalysis and combustion. The relation between both the reactions are very complex involving the production and consumption of reactant species at different rates within the fluid and on the catalyst surface such as reactions occurring in combustion, catalysis and biochemical systems [20]. Merkin [21] investigated the isothermal model of homogeneous-heterogeneous reactions in viscous flow past a flat plate. Kameswaran *et al.* [22] analyzed the viscous flow past a porous stretching surface filled with nanofluid in the presence of homogeneous-heterogeneous reactions. Nandkeolyar *et al.* [23] examined the combined effects of MHD and heat generation of a nanofluid past a stretching sheet with homogeneous-heterogeneous reactions and obtained the numerical solutions of two types of nanofluid including copper and gold nanoparticles. The mix convective flow near a stagnation-point of a nanofluid towards a stretching sheet in the presence of thermal radiation and homogeneous-heterogeneous reactions was investigated by Das *et al.* [24]. Recently, Hayat *et al.* [25] studied the boundary-layer flow of a carbon nanotubes near a stagnation point towards a porous stretching cylinder with homogeneous-heterogeneous reactions.

The aim of this study is to consider the combined effects of thermal radiation and homogeneous-heterogeneous reactions of a Cu-water nanofluid past a porous shrinking cylinder. The dual similar solutions of transformed non-linear equations are obtained using bvp4c. To the best of author's knowledge, no one yet considered this kind of problem.

Mathematical formulation

Consider the axi-symmetric flow of a Cu-water nanofluid towards a porous shrinking cylinder with homogeneous-heterogeneous reactions. Here $u_w(x) = cx/L$ is the variable shrink-

ing velocity, and L – the characteristics length. We considered a simple model of homogeneous-heterogeneous reactions as suggested by Chaudhary and Merkin [26]:

$$A + 2B \rightarrow 3B, \quad \text{rate} = k_c ab^2 \tag{1}$$

while for the catalyst surface, the first-order isothermal single reaction is described:

$$A \rightarrow B, \quad \text{rate} = k_p a \tag{2}$$

Here a and b are the chemical concentrations species A and B, respectively, whilst k_c and k_p are constants. It is presumed that both the processes of reaction are isothermal. Under the previous assumptions and boundary-layer approximation, the basic equations of nanofluid are:

$$\frac{\partial (ru)}{\partial x} + \frac{\partial (rv)}{\partial r} = 0 \tag{3}$$

$$u \frac{\partial u}{\partial x} + v \frac{\partial u}{\partial r} = \frac{\mu_{nf}}{\rho_{nf}} \left(\frac{\partial^2 u}{\partial r^2} + \frac{1}{r} \frac{\partial u}{\partial r} \right) \tag{4}$$

$$u \frac{\partial T}{\partial x} + v \frac{\partial T}{\partial r} = \frac{k_{nf}}{(\rho c_p)_{nf}} \left(\frac{\partial^2 T}{\partial r^2} + \frac{1}{r} \frac{\partial T}{\partial r} \right) - \frac{1}{r(\rho c_p)_{nf}} \frac{\partial}{\partial r} (rq_r) \tag{5}$$

$$u \frac{\partial a}{\partial x} + v \frac{\partial a}{\partial r} = D_A \left(\frac{\partial^2 a}{\partial r^2} + \frac{1}{r} \frac{\partial a}{\partial r} \right) - k_c ab^2 \tag{6}$$

$$u \frac{\partial b}{\partial x} + v \frac{\partial b}{\partial r} = D_B \left(\frac{\partial^2 b}{\partial r^2} + \frac{1}{r} \frac{\partial b}{\partial r} \right) + k_c ab^2 \tag{7}$$

The suitable boundary conditions are:

$$u = -u_w(x), \quad v = -V_w, \quad T = T_w, \quad D_A \frac{\partial a}{\partial r} = k_p a, \quad D_B \frac{\partial b}{\partial r} = -k_p a, \quad \text{at} \quad r = R$$

$$u \rightarrow 0, \quad T \rightarrow T_\infty, \quad a \rightarrow a_0, \quad b \rightarrow 0 \quad \text{as} \quad r \rightarrow \infty \tag{8}$$

where r is the co-ordinate measured in the radial direction, u and v – are components of velocity in x- and r-direction, respectively, μ_{nf} and ρ_{nf} – are the viscosity and density of the nanofluids, respectively, T is the temperature, T_∞ – the free stream temperature, D_A and D_B – are diffusion species coefficients of A and B, respectively, a_0 is the positive constant, k_{nf} – the thermal conductivity of nanofluid, and $(\rho c_p)_{nf}$ – the specific heat capacitance of nanofluid, which are defined:

$$\rho_{nf} = (1-\phi)\rho_f + \phi \rho_s, \qquad \frac{k_{nf}}{k_f} = \frac{(k_s + 2k_f) - 2\phi(k_f - k_s)}{(k_s + 2k_f) + \phi(k_f - k_s)}$$

$$\mu_{nf} = \frac{\mu_f}{(1-\phi)^{2.5}}, \qquad (\rho c_p)_{nf} = (1-\phi)(\rho c_p)_f + \phi(\rho c_p)_s \tag{9}$$

Here k_f and k_s are the thermal conductivities of the fluid and of the solid fractions, respectively, ϕ is the solid volume fraction of nanoparticles, ρ_f and ρ_s – are the densities of the fluid and of the solid fractions, respectively. Following Hayat *et al.* [18], the radiative heat flux q_r is expressed:

$$q_r = -\frac{16\sigma^* T_\infty^3}{3k^*}\frac{\partial T}{\partial r} \tag{10}$$

Now, we introduce the similarity transformation:

$$\eta = \frac{r^2 - R^2}{2R}\sqrt{\frac{c}{Lv_{\mathrm{f}}}}, \qquad \psi = \sqrt{\frac{cv_{\mathrm{f}}}{L}}xRf(\eta), \qquad \theta(\eta) = \frac{T - T_\infty}{T_w - T_\infty}$$

$$g(\eta) = \frac{a}{a_0}, \qquad h(\eta) = \frac{b}{a_0} \tag{11}$$

where η is the similarity variable, v_{f} – the kinematic viscosity of the base fluid, and ψ – the stream function defined:

$$u = \frac{1}{r}\frac{\partial \psi}{\partial r}, \quad v = -\frac{1}{r}\frac{\partial \psi}{\partial x}$$

which identically satisfied the equation of continuity (3). In view of relation (11), eqs. (4)-(10) are transformed into the following ODE:

$$\frac{1}{(1-\phi)^{2.5}\left(1-\phi+\phi\dfrac{\rho_{\mathrm{s}}}{\rho_{\mathrm{f}}}\right)}\Big[(1+2\gamma\eta)f''' + 2\gamma f''\Big] + ff'' - f'^2 = 0 \tag{12}$$

$$\frac{k_{\mathrm{nf}}}{k_{\mathrm{f}}}\Big[(1+2\gamma\eta)\theta'' + 2\gamma\theta'\Big] + \Pr\left(\frac{3N}{3N+4}\right)\left[1-\phi+\phi\frac{(\rho c_p)_{\mathrm{s}}}{(\rho c_p)_{\mathrm{f}}}\right]f\theta' = 0 \tag{13}$$

$$\frac{1}{\mathrm{Sc}}\Big[(1+2\gamma\eta)g'' + 2\gamma g'\Big] + fg' - Kgh^2 = 0 \tag{14}$$

$$\frac{\delta}{\mathrm{Sc}}\Big[(1+2\gamma\eta)h'' + 2\gamma h'\Big] + fh' + Kgh^2 = 0 \tag{15}$$

The transformed boundary conditions are:

$$f(0) = S, \quad f'(0) = -1, \quad \theta(0) = 1, \quad g'(0) = K_p g(0), \quad \delta h'(0) = -K_p g(0)$$

$$f'(\infty) \to 0, \quad \theta(\infty) \to 0, \quad g(\infty) \to 1, \quad h(\infty) \to 0 \tag{16}$$

where prime denote differentiation with respect to η, $\gamma = (Lv_{\mathrm{f}}/cR^2)^{1/2}$ – the curvature parameter, $\Pr = v_{\mathrm{f}}/\alpha_{\mathrm{f}}$ – the Prandtl number, $K = k_c a_0^2 L/c$ – the strength of homogeneous reaction parameter, $K_p = [k_p(Lv_{\mathrm{f}}/c)^{1/2}]/D_A$ – the strength of heterogeneous reaction parameter, $\delta = D_B/D_A$ – the ratio of mass diffusion coefficients, $\mathrm{Sc} = v_{\mathrm{f}}/D_A$ – the Schmidt number, and $S = V_w(L/cv_{\mathrm{f}})^{1/2} > 0$ – the suction parameter.

Further, it is presumed that the diffusion coefficients of concentrations species A and B are of a similar size. This leads to additional supposition that the diffusion coefficients D_A and D_B are identical *i. e.* $\delta = 1$ [22] and thus:

$$g(\eta) + h(\eta) = 1 \tag{17}$$

Previous assumption leads to reduce the eqs. (14) and (15) to:

$$\frac{1}{\text{Sc}}\left[(1+2\gamma\eta)g'' + 2\gamma g'\right] + fg' - Kg(1-g)^2 = 0 \tag{18}$$

subject to the boundary condition:

$$g'(0) = K_p g(0), \quad g(\infty) \to 1 \tag{19}$$

The quantities of physical interest are the skin friction coefficient $f''(0)$ and the local Nusselt number $-\theta'(0)$.

Stability analysis

As suggested by Merkin [27] and Weidman *et al.* [28], we test the stability analysis by taking the unsteady form of eqs. (4)-(7), see Khan *et al.* [29]:

$$\frac{\partial(ru)}{\partial x} + \frac{\partial(rv)}{\partial r} = 0 \tag{20}$$

$$\frac{\partial u}{\partial t} + u\frac{\partial u}{\partial x} + v\frac{\partial u}{\partial r} = \frac{\mu_{nf}}{\rho_{nf}}\left(\frac{\partial^2 u}{\partial r^2} + \frac{1}{r}\frac{\partial u}{\partial r}\right) \tag{21}$$

$$\frac{\partial T}{\partial t} + u\frac{\partial T}{\partial x} + v\frac{\partial T}{\partial r} = \frac{k_{nf}}{(\rho c_p)_{nf}}\left(\frac{\partial^2 T}{\partial r^2} + \frac{1}{r}\frac{\partial T}{\partial r}\right) - \frac{1}{r(\rho c_p)_{nf}}\frac{\partial}{\partial r}(rq_r) \tag{22}$$

$$\frac{\partial a}{\partial t} + u\frac{\partial a}{\partial x} + v\frac{\partial a}{\partial r} = D_A\left(\frac{\partial^2 a}{\partial r^2} + \frac{1}{r}\frac{\partial a}{\partial r}\right) - k_c ab^2 \tag{23}$$

$$\frac{\partial b}{\partial t} + u\frac{\partial b}{\partial x} + v\frac{\partial b}{\partial r} = D_B\left(\frac{\partial^2 b}{\partial r^2} + \frac{1}{r}\frac{\partial b}{\partial r}\right) + k_c ab^2 \tag{24}$$

where *t* represents the time. This introduce a new variable in similarity transformation:

$$\eta = \frac{r^2 - R^2}{2R}\sqrt{\frac{c}{Lv_f}}, \quad \psi = \sqrt{\frac{cv_f}{L}}xRf(\eta,\tau), \quad \theta(\eta,\tau) = \frac{T - T_\infty}{T_w - T_\infty}$$

$$g(\eta,\tau) = \frac{a}{a_0}, \quad h(\eta,\tau) = \frac{b}{a_0}, \quad \tau = \frac{c}{L}t \tag{25}$$

Employing eq. (25) in eqs. (21)-(24), we get:

$$\frac{1}{(1-\phi)^{2.5}\left(1-\phi+\phi\frac{\rho_s}{\rho_f}\right)}\left[(1+2\gamma\eta)\frac{\partial^3 f}{\partial\eta^3} + 2\gamma\frac{\partial^2 f}{\partial\eta^2}\right] + f\frac{\partial^2 f}{\partial\eta^2} - \left(\frac{\partial f}{\partial\eta}\right)^2 - \frac{\partial^2 f}{\partial\varpi\partial\eta} = 0 \tag{26}$$

$$\frac{k_{nf}}{k_f}\left[(1+2\gamma\eta)\frac{\partial^2\theta}{\partial\eta^2} + 2\gamma\frac{\partial\theta}{\partial\eta}\right] + \Pr\left(\frac{3N}{3N+4}\right)\left[1-\phi+\phi\frac{(\rho c_p)_s}{(\rho c_p)_f}\right]f\frac{\partial\theta}{\partial\eta} -$$

$$-\Pr\left(\frac{3N}{3N+4}\right)\left[1-\phi+\phi\frac{(\rho c_p)_s}{(\rho c_p)_f}\right]\frac{\partial\theta}{\partial\tau} = 0 \tag{27}$$

$$\frac{1}{Sc}\left[(1+2\gamma\eta)\frac{\partial^2 g}{\partial\eta^2}+2\gamma\frac{\partial g}{\partial\eta}\right]+f\frac{\partial g}{\partial\eta}-Kgh^2-\frac{\partial g}{\partial\tau}=0 \tag{28}$$

$$\frac{\delta}{Sc}\left[(1+2\gamma\eta)\frac{\partial^2 h}{\partial\eta^2}+2\gamma\frac{\partial h}{\partial\eta}\right]+f\frac{\partial h}{\partial\eta}+Kgh^2-\frac{\partial h}{\partial\tau}=0 \tag{29}$$

with the boundary conditions:

$$f(0,\tau)=S, \quad \frac{\partial f}{\partial\eta}(0,\tau)=-1, \quad \theta(0,\tau)=1, \quad \frac{\partial g}{\partial\eta}(0,\tau)=K_p g(0,\tau)$$

$$\delta\frac{\partial h}{\partial\eta}(0,\tau)=-K_p g(0,\tau), \quad \frac{\partial f}{\partial\eta}(\infty,\tau)\to 0, \quad \theta(\infty,\tau)\to 0, \quad g(\infty,\tau)\to 1, \quad h(\infty,\tau)\to 0 \tag{30}$$

Further, using eq. (17) with $\delta=1$, eqs. (28) and (29) can be written:

$$\frac{1}{Sc}\left[(1+2\gamma\eta)\frac{\partial^2 g}{\partial\eta^2}+2\gamma\frac{\partial g}{\partial\eta}\right]+f\frac{\partial g}{\partial\eta}-Kg(1-g)^2-\frac{\partial g}{\partial\tau}=0 \tag{31}$$

along with the condition:

$$\frac{\partial g}{\partial\eta}(0,\tau)=K_p g(0,\tau), \qquad g(\infty,\tau)\to 1 \tag{32}$$

According to Merkin [27] and Weidman *et al.* [28], stability of multiple solutions of the steady flow solution $f(\eta)=f_0(\eta)$, $\theta(\eta)=\theta_0(\eta)$, and $g(\eta)=g_0(\eta)$ satisfying the boundary value problems (12), (13), (16), (18), and (19), we write:

$$f(\eta,\tau)=f_0(\eta)+e^{-\alpha\tau}F(\eta,\tau)$$
$$\theta(\eta,\tau)=\theta_0(\eta)+e^{-\alpha\tau}\Theta(\eta,\tau) \tag{33}$$
$$g(\eta,\tau)=g_0(\eta)+e^{-\alpha\tau}G(\eta,\tau)$$

where α is an unknowwn eigenvalue (growth and decay distribution). Here $F(\eta,\tau)$, $\Theta(\eta,\tau)$, and $G(\eta,\tau)$, are small relative to $f_0(\eta)$, $\theta_0(\eta)$, and $g_0(\eta)$. Substituting eqs. (33) into eqs. (26), (27), and (31), we get the following linearized system:

$$\frac{1}{(1-\phi)^{2.5}\left(1-\phi+\phi\dfrac{\rho_s}{\rho_f}\right)}\left[(1+2\gamma\eta)\frac{\partial^3 F}{\partial\eta^3}+2\gamma\frac{\partial^2 F}{\partial\eta^2}\right]-2f_0'\frac{\partial F}{\partial\eta}+Ff_0''+$$

$$+f_0\frac{\partial^2 F}{\partial\eta^2}-\frac{\partial^2 F}{\partial\tau\partial\eta}+\alpha\frac{\partial F}{\partial\eta}=0 \tag{34}$$

$$\frac{k_{nf}}{k_f}\left[(1+2\gamma\eta)\frac{\partial^2\Theta}{\partial\eta^2}+2\gamma\frac{\partial\Theta}{\partial\eta}\right]+Pr\left(\frac{3N}{3N+4}\right)\left[1-\phi+\phi\frac{(\rho c_p)_s}{(\rho c_p)_f}\right]\cdot$$

$$\cdot\left(f_0\frac{\partial\Theta}{\partial\eta}+F\theta_0'+\alpha\Theta-\frac{\partial\Theta}{\partial\tau}\right)=0 \tag{35}$$

Zaib, A., *et al.*: Boundary-Layer Flow of a Cu-Water Nanofluid over a ...
THERMAL SCIENCE: Year 2019, Vol. 23, No. 1, pp. 295-306

301

$$\frac{1}{\mathrm{Sc}}\left[(1+2\gamma\eta)\frac{\partial^2 G}{\partial\eta^2}+2\gamma\frac{\partial G}{\partial\eta}\right]+f_0\frac{\partial G}{\partial\eta}+Fg_0'+4Kg_0G-3Kg_0^2G-$$

$$-KG+\alpha G-\frac{\partial G}{\partial\tau}=0 \tag{36}$$

with the boundary conditions:

$$F(0,\tau)=0, \quad \frac{\partial F}{\partial\eta}(0,\tau)=0, \quad \Theta(0,\tau)=0, \quad \frac{\partial G}{\partial\eta}(0,\tau)=K_p G(0,\tau)$$

$$\frac{\partial F}{\partial\eta}(\infty,\tau)\to 0, \quad \Theta(\infty,\tau)\to 0, \quad G(\infty,\tau)\to 0 \tag{37}$$

To determine the initial growth or decay of steady flow (33), we take $\tau=0$ and hence $F=F_0(\eta)$, $\Theta=\Theta_0(\eta)$, and $G=G_0(\eta)$ identify the initial growth or decay. Therefore, we have to solve the following eigen value problem to test our numerical procedure:

$$\frac{1}{(1-\phi)^{2.5}\left(1-\phi+\phi\dfrac{\rho_s}{\rho_f}\right)}\left[(1+2\gamma\eta)F_0'''+2\gamma F_0''\right]-2f_0'F_0'+F_0 f_0''+f_0 F_0''+\alpha F_0'=0 \tag{38}$$

$$\frac{k_{\mathrm{nf}}}{k_{\mathrm{f}}}\left[(1+2\gamma\eta)\Theta_0''+2\gamma\Theta_0'\right]+\mathrm{Pr}\left(\frac{3N}{3N+4}\right)\left[1-\phi+\phi\frac{(\rho c_p)_s}{(\rho c_p)_f}\right]\cdot$$

$$\cdot\left(f_0\Theta_0'+F_0\theta_0'+\alpha\Theta_0\right)=0 \tag{39}$$

$$\frac{1}{\mathrm{Sc}}\left[(1+2\gamma\eta)G_0''+2\gamma G_0'\right]+f_0 G_0'+F_0 g_0'+4Kg_0 G_0-3Kg_0^2 G_0-KG_0+\alpha G_0=0 \tag{40}$$

along with the following boundary conditions:

$$F_0(0)=0, \quad F_0'(0)=0, \quad \Theta_0(0)=0, \quad G_0'(0)=K_p G_0(0),$$

$$F_0'(\infty)\to 0, \quad \Theta_0(\infty)\to 0, \quad G_0(\infty)\to 0 \tag{41}$$

For the fixed values of the physical parameters, the stability is determined by the smallest eigen value of the corresponding steady flow solution $f_0(\eta)$, $\theta_0(\eta)$, and $g_0(\eta)$. As it has been suggested by Harris *et al.* [30], the possible range of eigen values can be obtained by relaxaing the boundary condition on $F_0(\eta)$, $\Theta_0(\eta)$ or $G_0(\eta)$. For the current problem, we relax the condition that $F_0(\eta)\to 0$ as $\eta\to 0$. Therefore, for a fixed value of α we solve the system of eqs. (38)-(40) along with the new boundary consition $F_0''(0)=1$, which give an infinite set of eigen values $\alpha_1<\alpha_2<\alpha_3<.....$, if the smallest eigen value α_1 is positive ($\alpha_1\geq 0$) then there is an initial decay of disturbances and the flow is stable, and if α_1 is negative ($\alpha_1<0$) then there is an initial growth of disturbances, which indicates that the flow is unstable.

Results and discussion

The set of transformed non-linear eqs. (12), (13), and (18) along with the boundary conditions (16) and (19) were solved numerically using the bvp4c code from MATLAB. To clearly realize physical insight for boundary-layer flow of a nanofluid in presence of homogeneous-heterogeneous reactions, the obtained numerically results for the skin friction coefficient

302

Zaib, A., *et al.*: Boundary-Layer Flow of a Cu-Water Nanofluid over a ...
THERMAL SCIENCE: Year 2019, Vol. 23, No. 1, pp. 295-306

Table 1. Thermophysical properties of fluid and nanoparticles

Physical properties	Fluid phase (water)	Cu
c_p [Jkg^{-1}K^{-1}]	4179	385
ρ [kgm^{-3}]	997.1	8933
k [Wm^{-1}K^{-1}]	0.613	400
$\alpha \cdot 10^{-7}$ [m^{2}s^{-1}]	1.47	1163.1

$f''(0)$, the heat transfer rate $-\theta'(0)$ as well as for velocity, temperature and concentration profiles are illustrated for different values of governing parameters involved in problem, viz., the nanovolume fraction, ϕ, the curvature parameter, γ, radiation parameter, N, strength of homogeneous reaction, K, and strength of heterogeneous reaction, K_p, in figs. 1-11. Following Oztop and Abu-Nada [31], the nanovolume fraction is from 0 to 0.2 in which $\phi = 0$ corresponds to the base fluid. The nanoparticles and the thermophysical properties of the base fluid are shown in tab. 1.

The effect of curvature, γ, on the velocity, temperature and concentration profiles are depicted in figs. 1-3, respectively. Figure 1 shows that the velocity profiles decreases with increasing γ for first solution and consequently, the momentum boundary-layer thickness increases. While the opposite effect is observed for second solution. Physically, this is due to the fact that an increase in the diameter of cylinder leads to decrease in the velocity of fluid within the boundary. On the other hand, the temperature profile increases with γ for first and second solutions as shown in fig. 2. This is due to fact that due to increase in the value of curvature parameter that leads to decrease in radius of cylinder which offers less resistance. Figure 3 shows that the concentration profiles decreases with increasing γ for first solution as well as for second solution and thus the concentration boundary-layer thickness becomes thicker and thicker for both solutions. It is also note from this figure that the second solution displays a thinner boundary-layer thickness compared to the first solution. Further, it is clear from these figures that the momentum, thermal and concentration boundary-layer thicknesses become larger for cylinder ($\gamma > 0$) compared to flat plate ($\gamma = 0$). It is worth mentioning that both solutions satisfy the for field boundary conditions asymptotically which support the validity of the results of the problem.
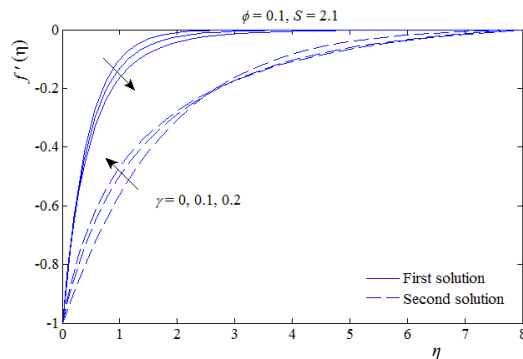
Figure 1. The velocity profiles for different values of γ
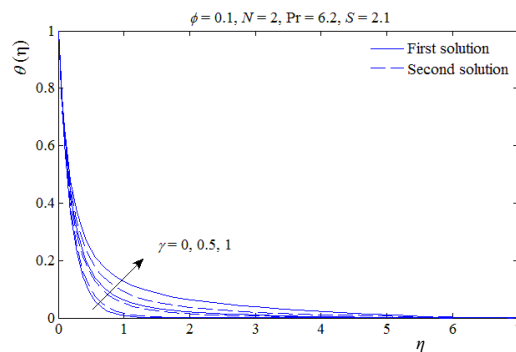
Figure 2. The temperature profiles for different values of γ

Figures 4-6 show the effect of nanoparticle volume fraction on the velocity, temperature and concentration profiles, respectively. Figure 4 shows that the velocity profiles increases with increasing values of ϕ and consequently decreases the momentum boundary-layer thickness for first solution, while the opposite trend is seen for second solution. This is because of the fact that the thermal conductivity increases by increasing the nanoparticle volume fraction which leads the further thinning of momentum boundary-layer. Figure 5 shows that the temperature profiles also increases with ϕ for first and second solutions and therefore, increases the thermal boundary-layer thickness. Since, the heat is transformed with faster rate from the sur-

Zaib, A., *et al.*: Boundary-Layer Flow of a Cu-Water Nanofluid over a ...
THERMAL SCIENCE: Year 2019, Vol. 23, No. 1, pp. 295-306

303

face of cylinder to the fluid and thus warms the region of thermal boundary-layer. It is also observed from this figure that the thickness of the boundary-layer is larger for Cu-water compare to pure water ($\phi = 0$). This is due to fact that thermal conductivity of Cu is high which in turns increases the thermal conductivity of fluid. Figure 6 shows that the concentration profiles increases with ϕ for first solution and decreases for second solution.
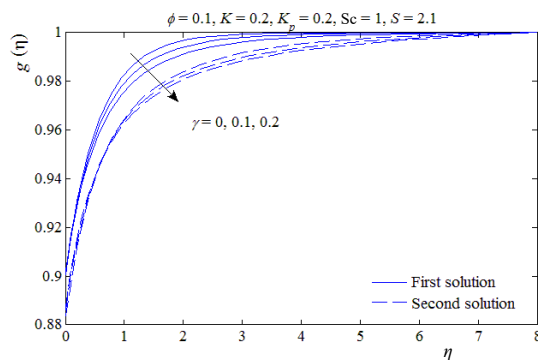
Figure 3. The concentration profiles for different values of γ
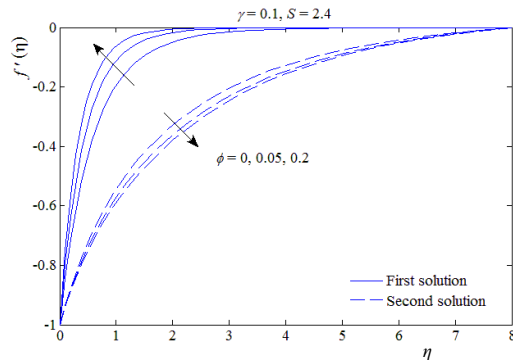
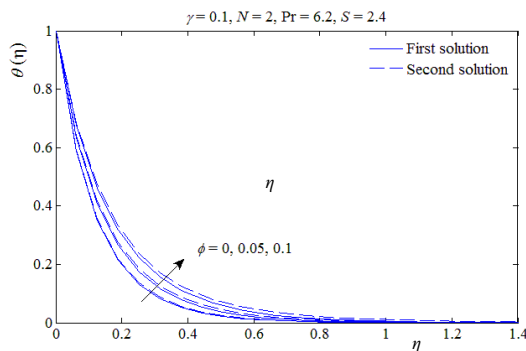**Figure 4. The velocity profiles for different values of ϕ**

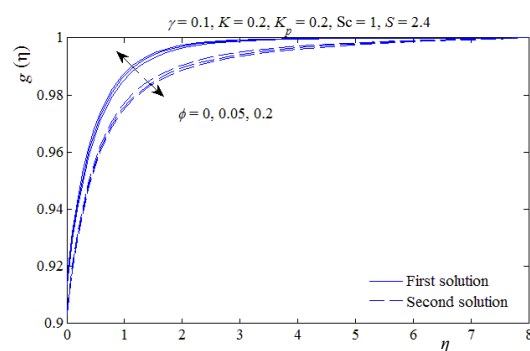**Figure 5. The temperature profiles for different values of ϕ**

Figure 6. The concentration profiles for different values of ϕ

Figure 7 shows the temperature profiles for different values of radiation parameter N. The results showed that the temperature profiles decreases with increasing N for first and second solutions. Thus, the thickness of thermal boundary-layer becomes thinner and thinner in case of first and second solutions. This is because of the fact that the large values of radiation parameter implies the dominance of conduction and therefore decreasing the thermal boundary-layer thickness, despite of increasing the thermal conductivity of Cu nanoparticles. Figures 8 and 9 show the variation of concentration profile for different values of the homogeneous reaction, K, and heterogeneous reaction, K_p, respectively. Figures 8 and 9 show that the concentration profiles decreases with increasing K and K_p for first and second solutions and thus the boundary-layer thicknesses increase for both solutions. It is also seen from this figure that the boundary-layer thicknesses of reactant increase with η for first and second solutions, however after greater values of η, they coincide which means that the homogeneous-heterogeneous reactions have no effect on the concentration boundary-layer of the reactants. Further, it is seen
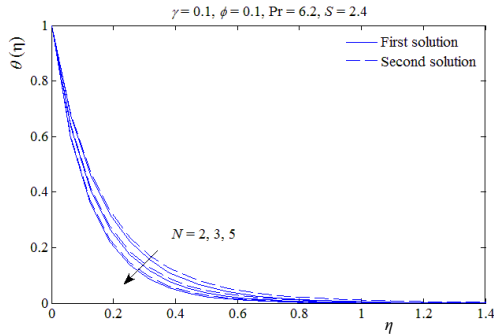
304

Zaib, A., *et al.*: Boundary-Layer Flow of a Cu-Water Nanofluid over a ...
THERMAL SCIENCE: Year 2019, Vol. 23, No. 1, pp. 295-306

Figure 7. The temperature profiles for different values of N

from fig. 8 that the second solution displays a thicker boundary-layer thickness compared to the first solution.

The skin friction coefficient, $f''(0)$, and the heat transfer rate, $-\theta'(0)$, against S for different values of γ are depicted in figs. 10 and 11, respectively. Figures 10 and 11 show that the values of $f''(0)$ and $-\theta'(0)$ decrease with increasing γ in case of first solution, whilst the values of $f''(0)$ and $-\theta'(0)$ increases for second solution. It is also observed from these figures that the values of $f''(0)$ and $-\theta'(0)$ are always 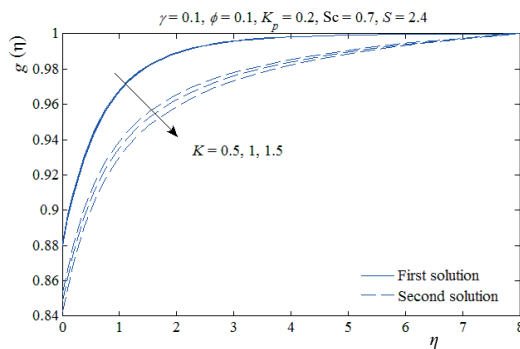positive which means that fluid exert a drag force on the cylinder and heat is moved from the hot cylinder to the cold fluid, respectively. Further, the dual similar solutions exist up to the critical value of suction parameter $S = \mathrm{Sc}(< 0)$ beyond which no solution exists. Based on our calculations, the critical values are 1.7010, 1.8000, and 1.9550 for $\gamma = 0, 0.1, 0.3$, respectively. Thus, the curvature parameter accelerate the boundary-layer separation.

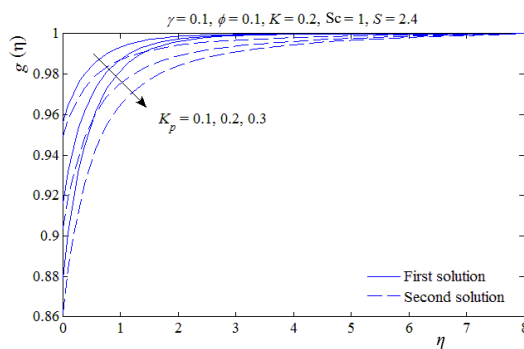**Figure 8. The concentration profiles for different values of K**

Figure 9. The concentration profiles for different values of K_p

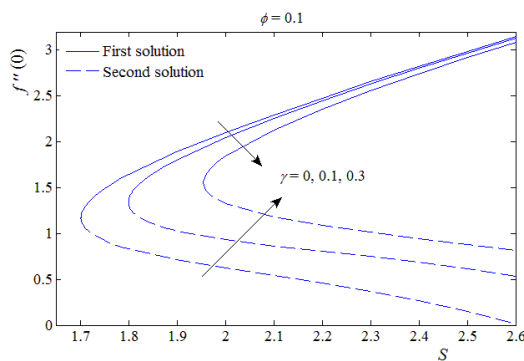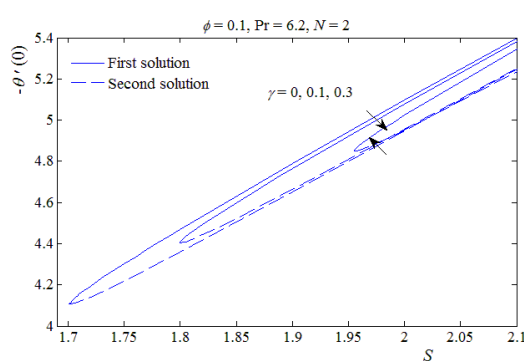**Figure 10. The values of $f''(0)$ *vs.* S for different values of γ**

Figure 11. The values of $-\theta'(0)$ *vs.* S for different values of γ

Zaib, A., *et al.*: Boundary-Layer Flow of a Cu-Water Nanofluid over a ...
THERMAL SCIENCE: Year 2019, Vol. 23, No. 1, pp. 295-306

305

Conclusions

In this research, the homogeneous-heterogeneous reactions on the flow of a Cu-water nanofluid past a permeable shrinking cylinder was studied numerically. Similarity solution of the transformed equations are obtained using bvp4c from MATLAB for different values of the governing parameters. From this study, the following conclusions could be drawn.

- Dual solutions are obtained for a certain range of suction parameter.
- The curvature parameter accelerate the boundary-layer separation.
- The velocity and concentration profiles increases due to nanoparticle volume fraction for first solution and decrease for second solution. While, the temperature profile increases with ϕ for both solutions.
- The concentration boundary-layer thickness increases with increasing homogeneous-heterogeneous reactions for first solution as well as for second solution.

Acknowledgement

References

[1] Choi, S. U. S., Enhancing Thermal Conductivity of Fluids with Nanoparticles, *Develop Appl. Non-New. Flows, 231* (1995), Oct., pp. 99-105
[2] Makinde, O. D., Aziz, A., Boundary Layer Flow of a Nanofluid Past a Stretching Sheet with a Convective Boundary Condition, *Int. J. Thermal Sci., 50* (2011), 7, pp. 1326-1332
[3] Mustafa, M., *et al.,* Stagnation-Point Flow of Nanofluid towars a Stretching Sheet, *Int. J. of Heat and Mass Transfer, 54* (2011), 25-26, pp. 5588-5594
[4] Hady, F. M., *et al.,* Radiation Effect on Viscous Flow of a Nanofluid and Heat Transfer over a Nonlinearly Stretching Sheet, *Nanoscale Res. Lett., 7* (2012), Dec., pp. 229-242
[5] Hamad, M. A. A., Ferdows, M., Similarity Solutions to Viscous Flow and Heat Transfer of Nanofluid over Nonlinearly Stretching Sheet, *Math. Mech. Eng. Ed., 33* (2012), 7, pp. 923-930
[6] Das, K., Mixed Convection Stagnation Point Flow and Heat Transfer of Cu-Water Nanofluids Towards a Shrinking Sheet, *Heat Tran. Asian Res., 42* (2013), 3, pp. 230-242
[7] Ibrahim, W., *et al.,* MHD Stagnation Point Flow and Heat Transfer Due to Nanofluid Towards a Stretching Sheet, *Int. J. Heat Mass Transfer,* 56 (2013), 1-2, pp. 1-9
[8] Mansur, S., *et al.,* The Magnetohydrodynamic Stagnation Point Flow of a Nanofluid over a Stretching/ Shrinking Sheet with Suction, *PloS ONE, 10* (2015), 3, pp. 1-14
[9] Hayat, T., *et al.,* Stagnation Point Flow of Carbon Nanotubes over Stretching Cylinder with Slip Conditions, *Open Phys., 13* (2015), 1, pp. 188-197
[10] Dhanai, R., *et al.,* Multiple Solutions of MHD Boundary Layer Flow and Heat Transfer Behavior of Nanofluids Induced by a Power-Law Stretching/Shrinking Permeable Sheet with Viscous Dissipation, *Powder Tech., 273* (2015), Mar., pp. 62-70
[11] Faiza, A. S., Effects of Radiation on Convection Heat Transfer of Cu-Water Nanofluid Past a Moving Wedge, *Thermal Science, 20* (2016), 2, pp. 437-447
[12] Wang, C. Y., Fluid Flow Due to a Stretching Cylinder, *Phys. Fluids, 31* (1988), 3, pp. 446-468
[13] Ishak, A., *et al.,* Uniform Suction/Blowing on Flow and Heat Transfer Due to a Stretching Cylinder, *Math. Model., 32* (2008), 10, pp. 2059-2066
[14] Mukhopadhyay, S., Chemically Reactive Solute Transfer in Boundary Layer Slip Flow Along a Stretching Cylinder, *Front. Chem. Sci. Eng., 5* (2011), 3, pp. 385-391
[15] Mukhopadhyay, S., MHD Boundary Layer Slip Flow along a Stretching Cylinder, *Ain Shams Eng. J., 4,* (2013), 2, pp. 317-324
[16] Bhattacharyya, K., Boundary Layer Flow and Heat Transfer over a Permeable Shrinking Cylinder with Mass Suction, *Int. J. of Applied Mechanic and Engineering, 18* (2013), 4, pp. 1003-1012
[17] Najib, N., *et al.,* Stagnation Point Flow and Mass Transfer with Chemical Reaction Past a Stretching/ Shrinking Cylinder, *Sci. Rep. 4* (2014), Feb., 4178

[18] Hayat, T., *et al.,* Flow of Variable Thermal Conductivity Fluid Due to Inclined Stretching Cylinder with Viscous Dissipation and Thermal Radiation, *Appl. Math. Mech. Eng. Ed., 35* (2014), 6, pp. 717-728

[19] Omar, N. S. *et al.,* Stagnation Point Flow over a Stretching or Shrinking Cylinder in a Copper-Water Nanofluid, *Indian J. Sci. Tech., 8* (2015), 31, pp. 1-7

[20] Hayat, T., *et al.,* Impact of Magnetohydrodynamics in Bidirectional Flow of Nanofluid Subject to Second Order Slip Velocity and Homogeneous-Heterogeneous Reactions, *J. Mag. Magnet. Mater., 395* (2015), Dec., pp. 294-302

[21] Merkin, J. H., A Model for Isothermal Homogeneous-Heterogeneous Reactions in Boundary Layer Flow, *Math. Comput. Model., 24* (1996), 8, pp. 125-136

[22] Kameswaran, P. K., *et al.,* Homogeneous-Heterogeneous Reactions in a Nanofluid Flow Due to a Porous Stretching Sheet, *Int. J. Heat Mass Transfer, 57* (2013), 2, pp. 465-472

[23] Nandkeolyar, R., *et al.,* Heat Transfer on Nanofluid Flow with Homogeneous-Heterogeneous Reactions and Internal Heat Generation, *J. Heat Transfer, 136* (2014), 12, 122001

[24] Das, M., *et al.,* Mixed Convection and Nonlinear Radiation in the Stagnation Point Nanofluid Flow Towards a Stretching Sheet with Homogenous-Heterogeneous Reactions Effects, *Procedia Eng., 127* (2015), Dec., pp. 1018-1025

[25] Hayat, T., *et al.,* Homogeneous-Heterogeneous Reactions in the Stagnation Point Flow of Carbon Nanotubes with Newtonian Heating, *AIP Advances, 5* (2015), 2, 027130

[26] Chaudhary, M. A., Merkin, J. H., A Simple Isothermal Model for Homogeneous-Heterogeneous Reactions in Boundary Layer Flow: I Equal Diffusivities, *Fluid Dyn. Res., 16* (1995), 6, pp. 311-333

[27] Merkin, J. H., On Dual Solution Occurring in Mixed Convection in a Porous Medium, *J. Eng. Math*., *20* (1985), 2, pp. 171-179

[28] Weidman, P. D., *et al*., The Effect of Transpiration on Self Similar Boundary Layer Flow over Moving Surfaces, *Int. J. Eng. Sci*., *44* (2006), 11-12, pp. 730-737

[29] Khan, M., *et al*., On Unsteady Heat and Mass Transfer in Carreau Nanofluid Flow over Expanding or Contracting Cylinder with Convective Surface Conditions, *J. Mol. Liq*., *231* (2017), Apr., pp. 474-484

[30] Harris, S. D., *et al*., Mixed Convection Boundary-Layer Flow Near the Stagnation Point on a Vertical Surface in a Porous Medium: Brinkman Model with Slip, *Transp. Porous Media*, *77* (2009), 2, pp. 267-285

[31] Oztop, H. F., Abu-Nada, E., Numerical Study of Natural Convection in Partially Heated Rectangular Enclosures Filled with Nanofluids, *Int. J. Heat Fluid Flow, 29* (2008), pp. 243-255